Design of a 3D-printed test rig for micro aerial robotics platforms

Natasha Botha[1*], *Willis* de Ronde[2], and *Beatrice* van Eden[2]

[1]Industry Connect, Future Production: Manufacturing, CSIR, South Africa
[2]Centre for Robotics and Future Production, Future Production: Manufacturing, CSIR, South Africa

Abstract. During the development of an aerial robotic platform, it is necessary to characterise the flight controller to ensure flight stability. Even though this can be done through open-source software like Betaflight, flight testing can result in potential crashes. To prevent this, this paper aims to design and manufacture a test rig to test and characterise the flight controller reliably. A 4-degree-of-freedom (DOF) test rig was developed to allow for vertical motion and characterise the yaw, pitch, and roll angles. It was also entirely constructed utilising additive manufacturing (AM). An iterative design approach was considered to improve the design after practical testing with a micro aerial robotic platform. This approach significantly enhanced the design of the ball joint and linear shaft to assist in better performance of the micro aerial robotic platform when using the test rig.

1 Introduction

Micro aerial robotics platforms have become quite popular in recent years due to their reliability, simplicity, economy (cost effective and easy to manufacture) and agility, with numerous commercial options available [1]. They are used in various different application areas such as educational platforms to teach the fundamentals of robotics [2], stocktaking, inspection, monitoring, and aerial mapping [1].

When developing a micro aerial robotics platform, it is required to characterise, or tune, the flight controller to improve flight stability. Similarly, to implement autonomous behaviour on the platform, a control algorithm must be developed and characterised. This leads to numerous crashes as the flight controller, or control algorithm, is tuned and flight tests are subsequently performed [1,3]. To prevent this, testing of either flight controller characterisation, or autonomous control algorithms, should be done in a controlled environment [1-3]. One way to achieve this is by having a test rig which allows for an easier transition between numerical and experimental analysis by evaluating the performance of the control algorithm in a safe, controlled environment, without any risk of collision [1-3].

In recent years, several different test rigs have been proposed in literature. The main difference between these design concepts is the number of degrees-of-freedom (DOF) which can be tested during control algorithm development and characterisation. These design concepts are illustrated in Figure 1.

* Corresponding author: nbotha1@csir.co.za

A 1-DOF test rig, Figure 1(a) only considers the rotation about a single axis with no translational movement. It therefore has limited functionality. Grzonka et al. [4] developed a test rig which only allows movement along a single axis to gain insights into the mapping between the command and the corresponding angle.

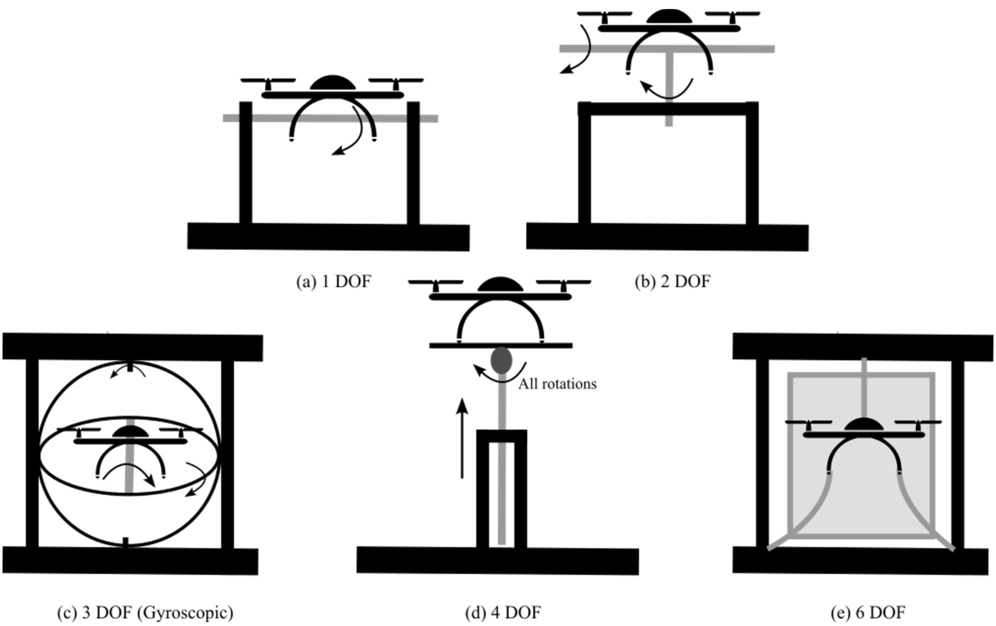

Fig. 1. Illustration of the design concepts of the control algorithm experimental test rigs for different DOF configurations.

A 2-DOF test rig only allows rotational movement along two axes, this design concept is illustrated in Figure 1(b). Poksawat and Wang [5] developed a 2-DOF test rig which allows rotational movement in the roll and yaw axis. They utilised the test rig to automatically characterise the control algorithm by conducting relay feedback control experiments in a controlled environment. Indoor and outdoor flight tests were then performed to verify the automatic tuning algorithm with stable attitude tracking.

A 3-DOF test rig is generally inspired by a gyroscopic, or gimbal, design as illustrated in Figure 1(c). Veyna et al. [2] developed a gyroscopic test rig for demonstration purposes when teaching control theory. Their design considered 3-DOF, that is the quadrotor can perform the pitch, yaw, and roll movements. They used Matlab Simulink to develop the aerial robotic control system and the implementation is tested via the gyroscopic test rig. On the other hand, Ucgun et al. [3] and Yüzgec et al. [6] developed a 3-DOF gyroscopic test rig considering different types and sizes of multirotors and therefore included a pulley and balance weight system to accommodate for altitude testing. An advantage of this design is that there is no motion restriction along the three rotational axes without altitude motion and is therefore a suitable rig for preflight tests to adjust any control parameters.

A 4-DOF allows for the rotational movements (roll, yaw and pitch) as well as a vertical translational movement as illustrated in Figure 1(d). Ömürlü et al. [7] designed a test rig using a universal joint to enable the rotational movement after a certain elevation level is achieved. They also ensured that some of the connecting elements, like the universal joint and roller bearings, were partially or fully lockable to allow for variation in the quadrotor mobility.

They compared the test rig results with those from a simulated environment for a basic PID controller.

A 6-DOF test rig, Figure 1(e), allows for motion similar to that in free flight, albeit with certain test limitations to avoid any potential crashes. Mukras and Omar [1] developed a test rig which utilises cables to restrict the area of flight and the cable length is chosen to allow limited movement along the translational and rotational axes. They designed their test rig to be multi-functional to include flight training, experimental determination of mass properties, and to test and characterise the performance of control algorithms. Their test rig also allows for the attachment of a suspended load to the multirotor. Jatsun et al. [8] designed a test rig which allows the quadcopter to travel a maximum distance of 2 m. In their design the quadrotor is mounted on a support which allows for the full range of translational motion, and a universal joint which allows for the rotational movements. This test setup allowed them to validate their hover control algorithm.

The importance of a test rig cannot be underestimated, and based on the literature, the type of test rig is designed with a specific application and quadrotor in mind. Botha et al. [9] developed a prototype micro aerial robotic platform for indoor applications using off-the-shelf local components. One of the challenges that arose was flight stability, which can only be addressed by characterising or tuning the flight controller through an open-source software called Betaflight. However, after tuning the flight controller, test flights often resulted in a crash that damaged the frame.

Therefore, this paper aims to design a test rig to assist with reliable flight controller tuning in a controlled and safe environment. A design requirement is that this test platform be completely 3D-printed and able to test the micro aerial robotic platform developed by Botha et al. [9]. An iterative design approach will be considered, and as such, the test rig will be tested with the micro aerial robotic platform to evaluate the stability and performance under controlled conditions and identify areas for improvement in the design. This involves assessing the test rig's ability to induce the movements of interest and measuring key parameters for comparison with subsequent designs. This information will guide further improvements in aerial robotic platform design and control systems.

Note that the test rig introduces additional factors such as added mass, stiction, and friction through components like the linear shaft and spherical joint. These elements inherently affect the rotational and vertical dynamics of the aerial robotic platform in ways that are not representative of free flight but are very similar. The linear shaft, for instance, adds mass (15g, less than some sensors that get tested) that dampens the vertical translational response and the friction from the joint introduces damping in both translational and rotational axes, which could lead to slower responses or reduced agility compared to free flight conditions.

However, the purpose of this test rig is not to perfectly replicate free flight but to provide a controlled environment for characterising, tuning, and testing flight controllers. The rig allows us to perform safe, repeatable tests that prevent damage to the drone and sensors during the early stages of controller tuning. It also allows us to detect and correct potential issues before testing the drone in natural flight conditions.

The discrepancies between rig-based tests and free flight are compensated for in three manners:

- Characterisation adjustment by factoring in the effects of added mass and friction by calculating the damping effects and mass-based reductions in thrust-to-acceleration gain.
- When tuning the flight controller on the rig, we use deliberately conservative gains to prevent over-tuning based on rig dynamics. Once the drone has been safely tested on the rig, further adjustments to the controller can be made during free flight tests, where fine-tuning is required to account for the rig's impact.

- Since we change sensors and drones on the rig, we use it to pre-test and verify different configurations without risking damage to the aerial platform or its components. While these tests may not fully replicate free-flight dynamics, they provide a valuable benchmark for understanding the system's performance before moving to actual flight.

2 Test rig development

A 6-DOF test rig system provides more freedom and flexibility in allowing for motion similar to that of a free flight. However, this study focuses on reliably characterising the flight controller to ensure stability. For this reason, either a 3-DOF or 4-DOF design would be sufficient to characterise the flight controller reliably. A 4-DOF test rig concept was selected because it has the full spectrum of rotational movements while considering vertical movement.

The system has a linear joint that allows motion in the vertical direction and a spherical joint that allows motion in the yaw, pitch, and roll directions. The test rig design followed an iterative process, refining the design with each subsequent test using the micro aerial drone platform to identify and resolve potential design issues.

2.1 Aerial robotic platform

The micro aerial robotic platform developed by Botha et al. [9] is illustrated in Figure 2. The diagonal dimension of the cross frame is 184 mm and 130 mm between two motor mounting points. It has a total height of 69 mm with the camera payload housing. The initial frame was 3D printed using polyethylene terephthalate glycol (PETG) which has a Young's modulus of 3000 MPa and a yield strength of 53 MPa. The total weight of the platform is 172 g. T-motor F1303 motors were selected with a maximum thrust of 177 g according to the supplier datasheet. The aerial robotic platform motors were set to 70 % of the maximum throttle as the motors tend to burn out within seconds when operating at full throttle. The total thrust required for the aerial robotic platform is determined by:

$$\begin{aligned} total\ thrust\ required = {} & w_{total} \times power\!:\!weight \\ = {} & 172\ \times 2 \\ = {} & 344\ g \end{aligned} \tag{1}$$

To successfully ensure that the aerial platform can fly a total thrust of 344 g is required which is equivalent to 86 g per motor. At 70% throttle the motors produce a thrust of 60.2 g. The thrust to weight ratio at maximum thrust is therefore 1:0.97 and 1:2 at 70% throttle. For the flight controller a Matek F405-TE controller was selected, which has a built in IMU and barometer and configuration can be done via Betaflight with the *betaflight_4.4.2_STM32F405_MATEKF405TE_SD_9fe85f01* firmware. For more details regarding the selection of components and design of the aerial robotic platform the reader is referred to Botha et al. [9].

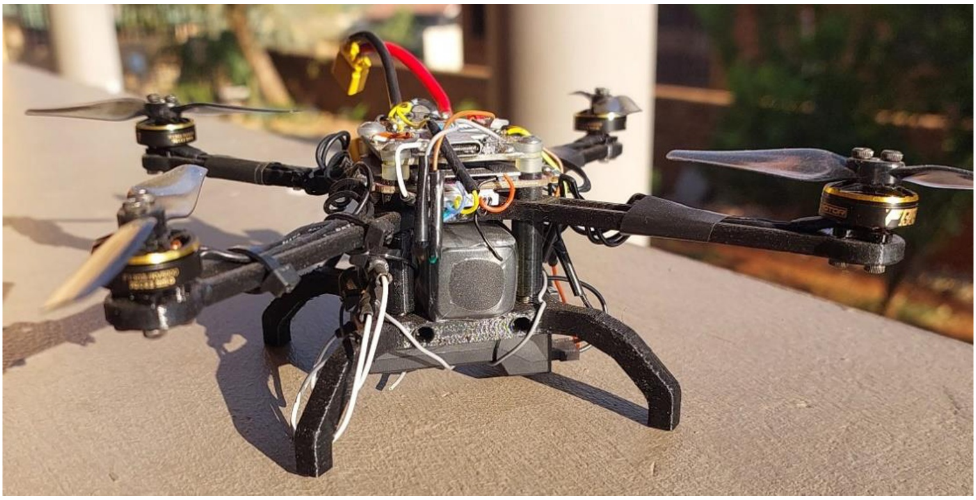

Fig. 2. Micro aerial robotic platform.

2.2 User requirements

A set of user requirements for creating a functional aerial robotic platform test rig is defined to enhance its capabilities. These specifications enable accurate simulation of conditions and precise data collection and serve as a foundation for analysing and improving the performance of the aerial robotic platform.

The development process for the test rig involves both mechanical design and data processing, each addressed separately to ensure clarity and focus. The mechanical design encompasses creating and refining the physical test rig, while data processing focuses on controlling the test rig, recording data, and ensuring consistency in testing conditions. This distinction allows for a thorough examination of each aspect, ensuring the test rig's overall functionality and effectiveness.

The following set of functional requirements were defined for the design and development of the test rig:

- The test rig should be able to induce controlled tilts in the pitch and roll axis at various angles to test the micro aerial robotic platform's ability to self-correct.
- The test rig must facilitate controlled movement around the yaw axis to test the aerial robotic platform’s rotational capability.
- The test rig must facilitate controlled vertical movements to test the aerial robotic platform’s ascent and descent capabilities.
- Build the test rig from robust polymer materials to withstand repeated use.
- Ensure the test rig is lightweight to facilitate easy transportation and setup, especially for testing small aerial robotic platforms.
- A modular design that allows for easy adjustment and reconfiguration of the test rig to accommodate different aerial robotic platform sizes and testing scenarios.
- Features to verify and ensure that each test is conducted under consistent conditions.
- A user-friendly and consistent setup for testing the aerial drone platform with the test rig.

2.3 Design process

The design process for the test rig involves several critical steps to ensure its functionality and effectiveness. Initially, the focus is on designing and prototyping the necessary mechanical setup. This phase includes creating a prototype to test the feasibility and practicality of the design. Once the prototype is built, it undergoes initial testing to validate its mechanical components and overall structure. Based on the results, necessary adjustments are made to fine-tune the test rig. The process then moves into an iterative improvement phase, where feedback from initial tests is used to enhance the test rig. Additional features may be implemented, and existing ones refined to better meet specific testing needs.

The system was designed using Siemens NX CAD software. An iterative design process was considered where the designed test rig was tested with a micro aerial robotic platform to determine its stability, reliability, and performance under controlled conditions. The linear movement, pitch, roll and yaw angles were tested to determine the test rig's capability and identify areas for improvement.

An initial prototype design for the 4-DOF test rig is illustrated in Figure 3. The test rig consists of a base with pillars attached to the linear guide. The linear shaft has a linear stopper attached at the bottom, limiting the aerial robotic platform's vertical flight. The linear shaft slides through the linear guide and connects to the spherical joint's socket, allowing for full rotation of the yaw angle and partial rotation of the roll and pitch angles. The spherical joint's ball fits into the socket and is attached to the mount, where the micro aerial robotic platform can easily be mounted for testing. The spherical joint consists of two parts that screw together to form a socket section around the ball.

The linear shaft is made from a metal tube as the initial 3D printed shaft tended to buckle and break with the weight of the aerial platform as it flew vertically. All other parts of the test rig were 3D printed using PLA.

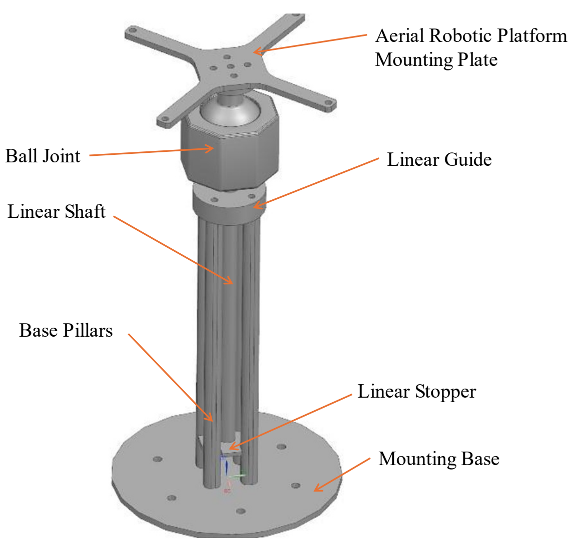

Fig. 3. CAD design of the prototype 4-DOF test rig concept.

2.4 Experimental testing

Data processing follows the successful creation of the mechanical prototype. This involves developing or integrating software, and data processing procedures, to control the aerial robotic platform, record data, and ensure consistency during testing. Ensuring that this procedure is compatible with Betaflight and Blackbox data formats is essential to facilitate seamless data collection and analysis.

The experimental testing aims to collect data from the micro aerial robotic platform [9] in a controlled environment using the developed test rig. This data collection will assist in evaluating the stability and performance of the test rig and improving the aerial robotic platform’s flight control and stability.

The test setup, illustrated in Figure 4, involved configuring the test rig in a controlled indoor environment to ensure stable temperature and wind conditions. Subsequent design iterations will also be tested using this same setup, under identical conditions and using the same micro aerial robotic platform for consistency.

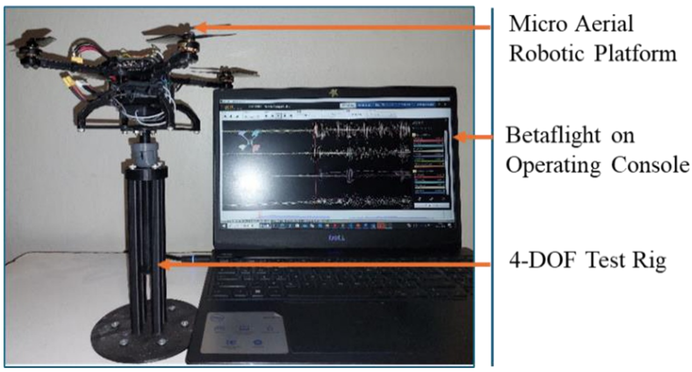

Fig. 4. Experimental test setup of the 4-DOF test rig and micro aerial robotic platform.

Data was collected via Betaflight and recorded on the flight controller using Blackbox. This study's parameters of interest were the tilt angles (pitch and roll), yaw angle, and motor throttle, which were recorded for each test flight. The maximum angle achieved during the induced tilt tests was measured for the tilt angles (Rig 1: 38°, Rig 2: 28°). The extent of yaw angles induced was also measured and analysed to determine the yaw stability and smoothness of the corrective action. The motor throttle was measured to provide an indication of the test rig’s capability to ensure linear movement of the aerial robotic platform.

When testing a drone test rig, several key measurements are crucial for assessing its performance, stability, and control. These include resultant force (vertical movement), yaw, pitch, and roll as illustrated in Figure 5. For the purposes of testing the test rig each of these aerial robotic platform movements will be considered in isolation to gain insight and understanding into the test rig’s ability to provide the desired movements.

In experimental testing, yaw, pitch, and roll angles are measured using gyroscope and accelerometer data, which are often processed by a state estimator like a complementary filter or Kalman filter. These filters help stabilise and accurately estimate the angle estimates.

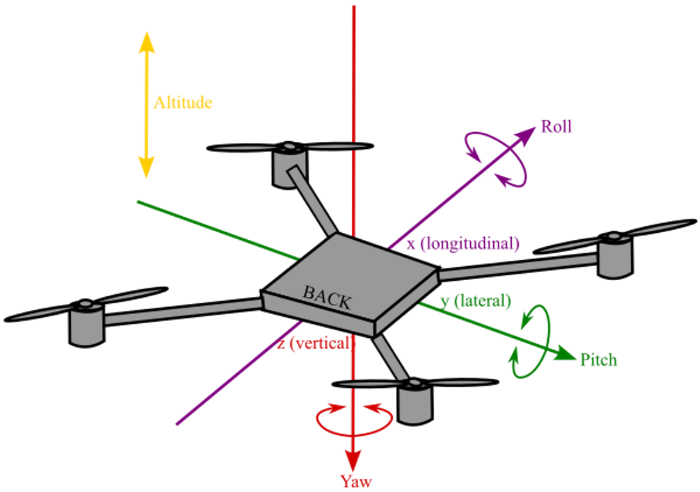

Fig. 5. Key measurements assessed for the performance, stability and control of a micro aerial robotic platform.

2.4.1 Resultant vertical force

The resultant force in the vertical direction, which is the sum of the upward thrust force and the downward gravitational force, is essential for understanding the aerial robotic platform's vertical stability and lift capabilities. Measuring this helps evaluate how well the aerial platform can maintain altitude, ascend, or descend in response to control inputs.

- **Upward Resultant Force** determines the aerial platform's ability to lift off. It's crucial for assessing motor power and efficiency.
- **Downward Resultant Force** is important for evaluating the platform's ability to descend smoothly and land safely.

Throttle Input directly controls the resultant force generated by the drone's motors. The throttle, in this case, represents the percentage of maximum power provided to the motors to lift the drone. In our tests, the motors were run at full power for maximum thrust generation, with the assumption that increased throttle results in increased vertical lift force. However, in typical flight conditions, the throttle is usually set to around 70% to avoid motor damage, and the drone's thrust is modulated accordingly.

2.4.2 Yaw

Yaw refers to the rotational movement around the vertical axis, which controls the aerial platform's orientation to the left or right. Measuring yaw is vital for assessing the platform's directional stability and control.

- **Yaw Stability** ensures the aerial robotic platform can maintain a set heading without unintended rotation.
- **Yaw Response** measures how quickly and accurately the platform can change its orientation in response to control inputs

We used a yaw rate controller for the yaw analysis, which means the Yaw Input represents a yaw rate reference rather than a yaw angle reference. Specifically, the input controls the rate at which the drone rotates about its vertical axis (i.e., its yaw rate). During the experimental tests, the Yaw Input was the maximum left or right yaw stick deflection, which commanded the drone to rotate at its maximum yaw rate. The test measured how quickly the drone could complete a 360° yaw rotation under this input. Thus:

- Yaw Input = Yaw rate reference

The controller adjusts the rotational velocity about the yaw axis, rather than directly controlling the yaw angle.

2.4.3 Pitch

Pitch involves the rotational movement around the lateral axis, affecting the aerial platform's forward and backward tilt. This measurement is essential for evaluating how well the platform can control its forward and backward motion.

- **Pitch Stability** indicates the platform's ability to maintain level flight without pitching excessively.
- **Pitch Response** assesses the platform's responsiveness to longitudinal (forward and backward) control inputs, which is crucial for longitudinal acceleration and deceleration.

In Betaflight, pitch and roll movements are measured using gyroscope and accelerometer data. The gyroscope measures the rate of angular change. At the same time, the accelerometer helps determine the drone's orientation relative to gravity. Betaflight uses these sensor readings to compute the drone's pitch and roll angles in real-time.

2.4.4 Roll

Roll refers to the rotational movement around the longitudinal axis, affecting the aerial platform's side-to-side tilt. Measuring roll is essential for evaluating lateral stability and control.

- **Roll Stability** ensures the platform can maintain level flight without rolling to the sides.
- **Roll Response** determines the platform's responsiveness to lateral (left and right) control inputs, which is crucial for lateral acceleration and deceleration, essential for avoiding obstacles and maintaining a stable flight path.

Similar to pitch movements, they are measured using gyroscope and accelerometer data.

3 Results and discussion

The initial prototype design of the 4-DOF test rig was 3D printed and tested with the micro aerial robotic platform. Two observations were made visually and were observed from the extracted data (see Figure 6):

1. The initial prototype had a large spherical joint that consisted of two parts that screwed together to form the socket section around the ball (see Figure 6(a)). During testing, it was noted that the large size of the spherical joint and metal linear shaft added excessive weight to the portion of the test rig lifted by the aerial robotic platform during flight. This lifted weight (27g) would not be present during normal flying conditions and must be kept to a minimum to keep test flights as close as possible to real flying conditions.
2. During testing, it was also noted that the aerial platform experienced problems when the pitch and roll angles were too large and required 100 % throttle to recover to the vertical position. These results will be discussed in detail in the relevant subsections. This is not an ideal situation in a free flight environment, as there are limitations on how long the motor can operate at 100 % throttle before burning out [9].

Based on these observations, a second version of the test rig focused on reducing the size of the spherical joint and redesigning the ball and socket to be a press fit shown in Figure 6(b). This redesign reduced the required parts, the overall weight and limited the roll and pitch angles to assist with testing. Even though the metal tube provided a smooth and sturdier vertical flight motion, it was decided to reduce the weight by 3D printing it for the redesign. To address the challenge of the 3D printed shaft which tended to buckle and break during initial tests, the new shaft was printed in a horizontal orientation so that the layer lines from the printing does not cause fault lines across the shaft. This orientation also ensures that the layer lines of the shaft and guide are not in the same direction, which could cause resistance to motion. The touching surfaces of the shaft and guide were also smoothed after 3D printing to ensure even motion. The shaft and the spherical joint were 3D printed using PETG with the remaining components 3D printed using PLA.

The 3D printed versions of both test rigs are shown in Figure 7 for comparison, where the orange circle highlights the biggest design change on the spherical joint. Note for the discussion of the results the initial prototype design and the redesigned test rig will be referred to as Rig 1 and Rig 2, respectively.

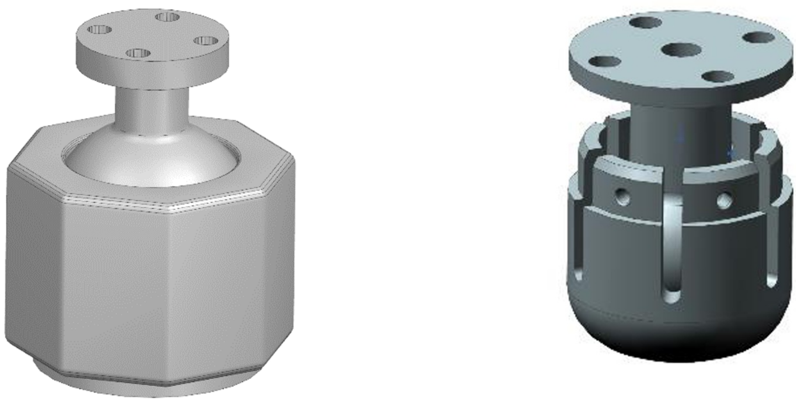

(a) Prototype (Rig 1) (b) Redesigned (Rig 2)

Fig. 6. CAD of the spherical joint of the (a) prototype (Rig 1) and (b) redesigned (Rig 2) test rigs.

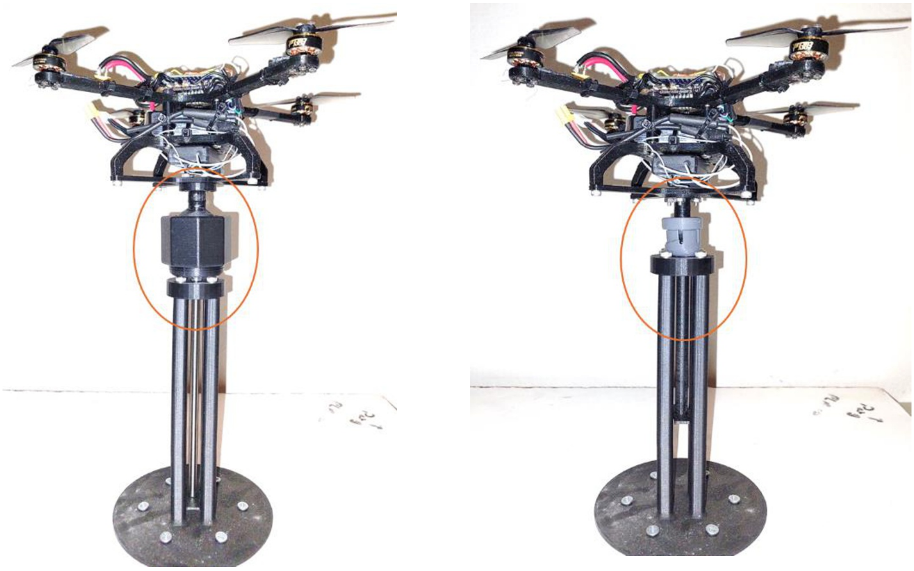

(a) Prototype (Rig 1) (b) Redesigned (Rig 2)

Fig. 7. 3D printed test rigs with the micro aerial vehicle mounted for the (a) prototype (Rig 1) and (b) redesigned (Rig 2) test rigs.

3.1 Thrust analysis

The thrust analysis provides insight into the vertical stability and lift capabilities of the aerial robotic platform and is measured by analysing the motor's throttle. For this analysis, the aerial robotic platform is flown only vertically, as far as possible, and the motor throttle required to move the platform upward is measured. The motor throttle was set to full power to achieve the required lift due to the additional weight of the linear shaft and spherical joint. However, during free flight, the motor throttle is set at 70 % to avoid damaging the motors as they can only sustain full throttle for 6 seconds before burning out [9]. The results for Rig 1 (green) and Rig 2 (blue) are shown in Figure 8.

Immediately evident is that Rig 1 required more throttle input to overcome the additional weight (from the linear shaft) as opposed to Rig 2. This is due to the differences in weight of the respective test rigs, where Rig 1 weighs approximately 63 g and Rig 2 weighs 24 g. The redesign of Rig 2 saw a reduction in overall weight of 61.9 %, which is mainly due to the spherical joint which requires less components and the linear shaft which was 3D printed for Rig 2 as opposed to the metal linear shaft used in Rig 1.

The metal linear shaft from Rig 1 remained sturdy and smooth throughout the tests. In contrast, the 3D printed linear shaft from Rig 2 tended to buckle towards the side when fully extended, resulting in a less smooth motion. This also prevented a smooth landing of the aerial platform as the linear shaft got stuck in the extended position. The linear shaft for Rig 2 is 3D printed, and slightly buckled to the side when extended fully. The performance of the linear shaft for Rig 2 improved once it was smoothed out, and a little grease was added.

Irrespective of the differences in weight, both test rigs showed that they were able to successfully move vertically up and down, and the motors therefore have enough power. In free flight, where the additional weight from the test rig will not be present, the aerial robotic platform should have a smooth vertical movement and lift off with no concerns over the motor's power and efficiency. However, there might be some corrections required to the PID control gains due to differences in mass (additional weight due to components lifted during flight on the test rig) and friction between the test rig setup and free flight.

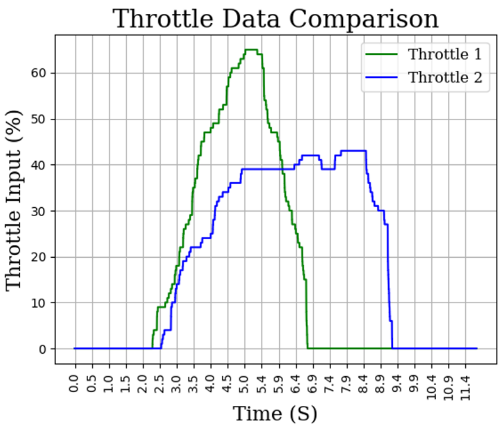

Fig. 8. Throttle input command from the aerial platform controller throttle stick.

3.2 Yaw analysis

The ability of the aerial robotic platform to rotate 360° anticlockwise with maximum yaw stick input to the left is illustrated in Figure 9. This provides an indication of the platform's directional stability and control.

In Figure 9(a) the setpoints are shown as the platform completes a 360° rotation and the platform was able to maintain a set heading without unintended rotations. The yaw stick input command is shown in Figure 9(b) where the same level of input is required for both test rigs to provide the same yaw rotational movement, and this input response was quick and accurate. For both figures the vertical drop at timestamp 14100 is indicative of the completion of the rotation where no further input from the toggle stick is provided.

The test flight was smooth and stable for both rigs indicating that both spherical joint designs are suitable for a yaw rotational motion. For Rig 1 the spherical joint can be tightened using the screw mechanism, making testing easier without incurring pitch or roll motions. Rig 2, on the other hand, has a clipping mechanism which still allows for pitch and roll motions. To prevent these motions and unwanted tilting, a piece of paper was added to the spherical joint to tighten the motion.

From these results both Rig 1 and Rig 2 followed a similar behaviour indicating that both test rigs can provide a smooth, stable and responsive yaw rotational movement.

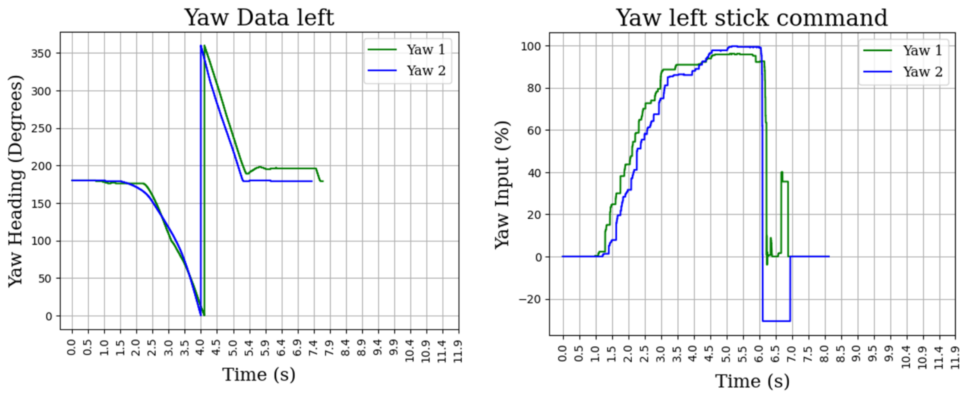

(a) Setpoint from flight controller (b) Input command from left toggle stick

Fig. 9. Yaw analysis results for the (a) setpoint from the flight controller and (b) input command from the transmitter left toggle stick for a 360° rotation.

3.3 Pitch analysis

For the pitch analysis, the rotational movement around the lateral axis was measured, which provides an indication of the aerial platform's control of its forward and backward tilting motion. The result for the pitch angle (in degrees) is presented in Figure 10(a) where the aerial platform was pitched backward before correcting it to achieve a vertical orientation. To achieve this, the spherical joint on Rig 1 was loosened to allow for rotation, while Rig 2 already allows this movement due to its design.

From Figure 10(a) the backward pitching angle starts at 9100 and ends at around 15100 before reaching the vertical position and pitching forward at around 17100. Rig 1 reached a pitch angle of -30° indicating the backwards motion, before returning to a vertical position. However, it subsequently pitched forward to an angle of 30° on its own due to the lower friction of the adjustable spherical joint mechanism. Rig 2 showed a similar behaviour, also achieving a pitch angle close to -30° before returning to the vertical position and pitching at an angle of around 15°. This indicates that the redesigned spherical joint with a clipping mechanism limited the forward pitching motion better than the prototype spherical joint with a screwing mechanism.

The correction, indicated by the forward pitching motion in Figure 10(a), required inputs for both the pitch and roll toggle sticks for the platform to achieve a vertical position is presented in Figure 10(b). At a timestep of 9100 the main input is from the pitching toggle for both test rigs, which is expected as only a pitching movement is induced. However, to achieve the vertical position only the pitch toggle stick is moved at first until a timestep of around 13100, before the roll toggle stick is also moved to achieve the vertical position. At a timestamp of 15100, the platform would start to move into the vertical position requiring some additional input from the roll toggle stick until around 17100. Rig 1 and Rig 2 both required roll and pitch inputs to achieve the vertical position, however Rig 1 needed a larger input which is attributed to the looser spherical joint with an adjustable mechanism which not only offers a larger range of rotational movement but is also larger than Rig 2's spherical joint. This behaviour is potentially due to the additional battery weight along the lateral axis, as well as the platform's centre of mass which might not align with the test rig's centre axis. This was also observed in the flight tests where the aerial platform flight was jerkier and required more command input from the operator to ensure the platform remains within the pitch motion and avoids going into a roll motion.

Rig 2 performed slightly better than Rig 1 mainly due to its smaller spherical joint with a clipping mechanism which limited the rotational movement and consequently the pitch angle. This also helped to reduce the impact of the battery's weight along the lateral axis. Both rigs were able to provide some stability of the aerial platform in the pitching movement, however correcting this required multiple inputs. The aerial platform was responsive in correcting the movements.

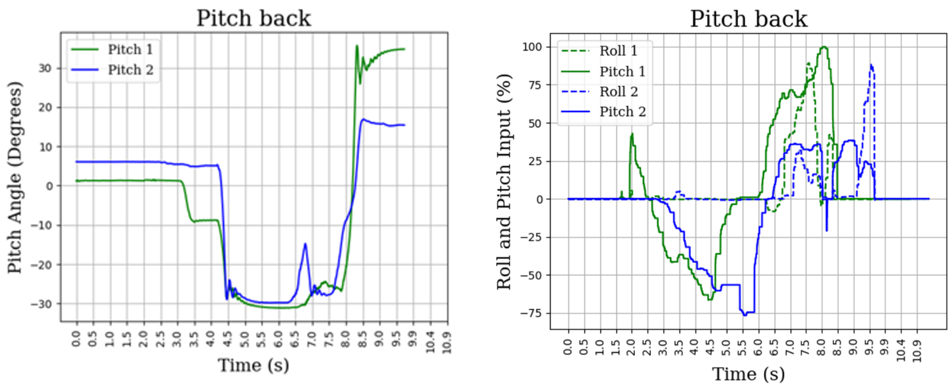

(a) Sensor values from flight controller (b) Input command from pitch toggle stick

Fig. 10. Pitch analysis results for the (a) sensor values from the flight controller and (b) input command from the transmitter pitch toggle stick for a backward motion.

3.4 Roll analysis

The roll analysis considered the rotational movement of the aerial robotic platform along the longitudinal axis which provides an indication of the platform's ability to move from side-to-side. The results are illustrated in Figure 11, with the roll angle provided in Figure 11(a) and the required input command from the roll toggle stick in Figure 11(b). Similar to the pitch analysis, the roll analysis first tilts the aerial platform to the right side, before correcting it back into the vertical position, ideally only using the roll toggle stick. To achieve this, the spherical joint on Rig 1 was loosened to allow for rotation, while Rig 2 already allows this movement due to its design.

From Figure 11(a) the aerial platform is rolled to the right around timestamp 9100 before correcting it at timestamp 16100 to its vertical position. Rig 1 achieved a roll angle of 30°, whereas Rig 2 achieved an angle of approximately 28°. However, Rig 1 subsequently rolled to the left to an angle of about -35° on its own after reaching the vertical position. This is likely due to the lower friction, as the spherical joint with the screwing mechanism was adjusted to a looser setting. Nevertheless, at a timestamp of 22100 the platform reached the vertical position requiring only input from the roll toggle stick as shown in Figure 11(b). In contrast, Rig 2 features a spherical connection with a clipping mechanism which took much longer and required more input from the roll toggle stick, Figure 11(b), to reach the vertical position. Due to the higher friction in the spherical joint, the platform did not roll to the left as observed with Rig 1. This behaviour, similar to the pitch analysis, was observed during the flight tests where the aerial robotic platform was jerkier in the roll motion and required additional input from the operator to correct.

Both test rigs were able to successfully perform the roll motion, however the type of spherical joint did play a role in the stability and responsiveness of the aerial platform to achieve its vertical position. Rig 2 provided better stability compared to Rig 1 as it reached its vertical position without tilting to the opposite side and requiring additional correction; and Rig 1 provided better responsiveness due to the lower friction of the spherical joint.

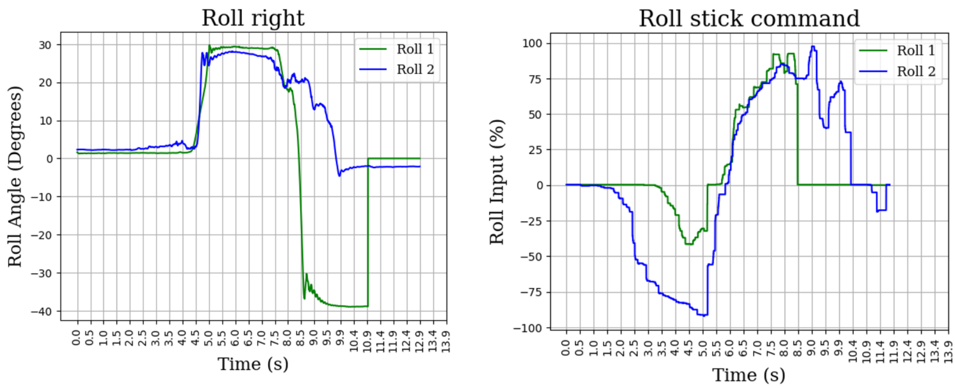

(a) Sensor values from flight controller (b) Input command from roll toggle stick

Fig. 11. Roll analysis results for the (a) sensor values from the flight controller and (b) input command from the transmitter roll toggle stick for a motion to the right side.

3.5 Conclusion

Both Rig 1 and Rig 2 met the functional requirements for the test rig as outlined in Section 2.1. They successfully facilitated controlled tilts in both the pitch and roll angles, yaw angle and vertical movements. They were both constructed from robust materials, ensuring durability, and designed to be lightweight for easy transportation and setup. Additionally, both rigs featured modular designs, allowing for easy adjustments and reconfiguration, and they provided a user-friendly setup for conducting tests in a controlled environment.

Rig 1 allows for the adjustment of the rotation resistance of the rig by loosening or tightening the spherical joint screw mechanism, but at the risk of stability to the aerial platform when correcting to a vertical position. Whereas Rig 2 limits the pitch and roll to shallower angles, but due to the higher fixed rotation resistance of the spherical joint it affected responsiveness. However, based on the test results, a few minor redesigns are proposed for each test rig to further optimise performance:

- **Rig 1:** While its spherical joint with a screwing mechanism positively affected rolling tests, the battery weight on the pitch axis in combination with the low friction joint negatively impacted pitching tests and increased the throttle requirement. A redesign to reduce its size and weight while retaining the adjustable screwing feature to control the roll and pitch angles, and friction would enhance its overall performance.
- **Rig 2:** The spherical joint with a clipping mechanism proved slightly advantageous during pitching tests but less effective for rolling. Maintaining its lower weight is beneficial, but exploring adjustable features for the spherical joint could improve its rolling performance. The 3D printed linear guide buckled when in the full vertical motion, and by considering a lightweight metal material for this component, the vertical motion of the drone will be improved.

It is recommended to further improve the design of Rig 2 by implementing a redesign of the spherical joint screwing mechanism from Rig 1, incorporating some of the design elements of the spherical joint from Rig 2, which was more advantageous for pitching. Implementing this proposed redesign would likely result in an optimised version of the test rig, achieving the best performance across all testing scenarios.

4 Conclusion

In this paper, a test rig design for a micro aerial robotic platform was proposed and was mostly 3D printed, except for the metal linear shaft for Rig 1. The 4-DOF test rig allowed for flight testing in the vertical direction, as well as testing the yaw, roll and pitch angles.

An iterative design approach with continuous testing was considered where the original prototype was tested with a micro aerial robotic platform. The prototype design consisted of a base with four pillars attached to a linear guide which housed the linear shaft with a stopper attached to limit vertical movement. The linear shaft connects to a spherical joint which consists of a ball and a socket which screws together allowing for flexibility in the rotational movement. The spherical joint is attached to a mounting plate where the aerial robotic platform is mounted. Visual observations from experimental tests provided insight into potential design changes for a second redesigned test rig. These mainly included reducing the size and weight of the spherical joint to improve the vertical movement, and limiting the rotational movement to prevent instances where the aerial platform could not self-correct after either pitching or rolling.

The performance of both test rigs was compared by measuring the motor throttle, roll, pitch and yaw angles. The original prototype provided more flexibility to control the angle of rotational movement with its screwing mechanism, but at the risk of stability of the aerial platform. Whereas the redesign limits the rotational movement, but due to the higher friction of the spherical joint it affected the platform's responsiveness. The reduced weight of the spherical joint was low enough that the aerial platform was able to lift off in the vertical direction with ease reducing the strain on the motors. These results indicated that there are advantages and disadvantages of both test rigs and that another design iteration is required.

It is recommended to redesign the spherical joint in the redesigned test rig to include features from the original prototype spherical joint screwing mechanism which allowed for more flexibility in the rotational movements and lower friction. The next iteration of the test rig should therefore retain and combine the positive design concepts from each test rig for an optimised version.

Nevertheless, flight testing with a test rig has indicated that the characterisation of the flight controller can be simplified. However, for free flight, characterisation results obtained from and controller gains tuned on the test rig will have to be adjusted to account for the additional weight and friction observed on the test rig. This initial PID tuning on the test rig does however give a good starting point for further optimisation in free flight, greatly reducing the risk of crashing. It also allowed for easy resolution of previously experienced issues, such as the communication challenges experienced between the transmitter and receiver.

Future work will include investigating the differences in the PID control between the test rig and free flight. This will include the development, and optimisation, of adjustment parameters.

References

1. S.M.S. Mukras, H.M. Omar, Development of a 6-DOF testing platform for multirotor flying vehicles with suspended loads, Aerospace, **8**, pp. 355 (2021).
2. U. Veyna, S. Garcia-Nieto, R. Simarro, J.V. Salcedo, *Quadcopters testing platform for educational environments*, Sensors, 21, pp. 4134 (2021).
3. H. Ücgün, I. Ökten, U. Yüzgec, M. Kesler, *Test platform and graphical user interface design for vertical take-off and landing drones*, Romanian Journal of Information Science and Technology, **25**, pp. 350 – 367 (2022).

4. S. Grzonka, G. Grisetti, W. Burgard, *A fully autonomous indoor quadrotor*, IEEE Transactions on Robotics, 28, pp. 90 – 100 (2012).
5. P. Poksawat, L. Wang, *Automatic tuning of hexacopter attitude control systems with experimental validation*, in Proceedings of International Conference on System Theory, Control and Computing, pp. 753 - 758 (2017).
6. U. Yüzgec, I. Ökten, H. Ücgün, A. Gün, T. Türkyilmaz, M. Kesler, C. Karakuzu, G. Ucar, *Development of the test platform for rotary wing unmanned air vehicle*, Bilecik Seyh Edebali Universitesi Fen Bilimleri Dergisi, **3**, pp. 18 – 24 (2016).
7. V.E. Ömürlü, A. Kirli, U. Büyüksahin, S.N. Engin, S. Kurtoglu, *A stationary, variable DOF flight control system for an unmanned quadrocopter*, Turkish Journal of Electrical Engineering and Computer Sciences, **19**, pp. 891 – 899 (2011).
8. S. Jatsun, O. Emelyanova, B. Lushnikov, A.S. Martinez-Leon, L.M. Mosquera-Morocho, A. Pechurin, C.A. Nolivos-Sarmiento, *Hovering control algorithm validation for a mobile platform using an experimental test bench*, IOP Conference Series: Materials Science and Engineering, 1027, pp. 012008 (2021).
9. N. Botha, B. van Eden, L. Lehman, J. Verster, *Prototype Design of an Aerial Robotic Platform for Indoor Applications*, in Proceedings of RAPDASA-Robmech-PRASA-AMI, 30 October – 2 November 2023, Pretoria, South Africa (2023).